MOLECULAR AND CELLULAR BIOLOGY, Jan. 1994, p. 587–596
0270-7306/94/$04.00+0

Vol. 14, No. 1

Selection for Arsenite Resistance Causes Reversible Changes in Minicircle Composition and Kinetoplast Organization in *Leishmania mexicana*

SHO TONE LEE,* HSING YIN LIU, SUE PING LEE, AND CHI TARN

Laboratory of Molecular Parasitology, Institute of Biomedical Sciences, Academia Sinica, Taipei 11529, Taiwan, Republic of China

Received 5 August 1993/Returned for modification 15 September 1993/Accepted 8 October 1993

Certain minor minicircle sequence classes in the kinetoplast DNA (kDNA) networks of arsenite- or tunicamycin-resistant *Leishmania mexicana amazonensis* variants whose nuclear DNA is amplified appear to be preferentially selected to replicate (S. T. Lee, C. Tarn, and K. P. Chang, Mol. Biochem. Parasitol. 58:187–204, 1993). These sequences replace the predominant wild-type minicircle sequences to become dominant species in the kDNA network. The switch from wild-type-specific to variant-specific minicircles takes place rapidly within the same network, the period of minicircle dominance changes being defined as the transition period. To investigate the structural organization of the kDNA networks during this transition period, we analyzed kDNA from whole arsenite-resistant *Leishmania* parasites by dot hybridization with sequence-specific DNA probes and by electron-microscopic examination of isolated kDNA networks in vitro. Both analyses concluded that during the switch of dominance the predominant wild-type minicircle class was rapidly lost and that selective replication of variant-specific minicircles subsequently filled the network step by step. There was a time during the transition when few wild-type- or variant-specific minicircles were present, leaving the network almost empty and exposing a species of thick, long, fibrous DNA which seemed to form a skeleton for the network. Both minicircles and maxicircles were found to attach to these long DNA fibrils. The nature of the long DNA fibrils is not clear, but they may be important in providing a framework for the network structure and a support for the replication of minicircles and maxicircles.

By now it is well accepted that the network structure of the kinetoplast DNA (kDNA) of trypanosomatids is formed through catenation of minicircles and maxicircles (24, 25, 28). Different forms of catenation of minicircles in the network have been suggested on the basis of electron-microscopic studies (1, 26). By using topoisomerase, the kDNA network can be unlinked into monomeric maxicircles and minicircles (4, 16, 21). Dissociation of kDNA networks with endonucleases specific to minicircles and maxicircles has led to the conclusion that minicircles are important in maintaining the network structure (6, 9, 10). Several reports have suggested, however, that kinetoplast DNA contains additional components other than individual maxicircles and minicircles (1, 8, 16). Such components include minicircle concatemers (3, 27) and linear DNA components (1, 12). However, because of the extreme crowding of the molecules within the intact network, the detailed organization of the network in its natural state has never been revealed by electron microscopy.

Recently we have reported that kDNAs from wild-type *Leishmania* cells show no apparent hybridization with those from variants made resistant to either arsenite or tunicamycin (15). Subsequent cloning and sequencing of kDNA maxicircles (14) and minicircles (13) from repeatedly cloned parasites before and after drug resistance selection indicate that the change in maxicircles is due to base replacements and insertion/deletion of nucleotide sequences whereas the change in minicircles is due to preferential selection of certain minor sequences of minicircles to replicate to become dominant species in the network. The switch in replication from one class of minicircle to another occurs within a narrow range of drug and in three to four passages during stepwise drug resistance selection (13). The switch is not due to selection of a particular parasite population bearing that specific class of minicircle but rather to a process during which the predominant wild-type minicircles are replaced by certain preexisting minor sequences to become dominant in the same network. This has been demonstrated by minicircle-specific endonuclease treatment combined with electron-microscopic examination of the kDNA networks (13). During such dynamic switching, the network structure is not disrupted, at least according to results of DAPI (4′,6′-diamidino-2-phenylindole) staining of the cells. In this study we took advantage of the transition period during the switch, in which neither wild-type- nor variant-specific minicircles were present in full strength, to explore the structural organization of the kDNA network.

MATERIALS AND METHODS

Parasites. Repeatedly cloned *Leishmania mexicana amazonensis* (LV78) promastigotes (clone 2-23) and its arsenite-resistant variants produced as described previously (13, 14) were grown at 27°C in medium 199 containing 20 mM *N*-2-hydroxyethylpiperazine-*N*′-2-ethanesulfonic acid (HEPES; pH 7.4), supplemented with 10% fetal bovine serum (inactivated at 56°C for 30 min), 100 Units of penicillin ml^{-1}, and 100 μg of streptomycin ml^{-1}. Sodium arsenite-resistant variants derived from clone 2-23 made resistant to 10 μM

* Corresponding author. Phone: 886-2-7899170. Fax: 886-2-7825573.

arsenite (A_{10} cells) by a serial stepwise selection were grown in 15 μM arsenite and passaged every 4 days continuously in the same drug concentration (13). These were designated A_{15} cells. The A_{15} cells had the same growth patterns as the wild-type cells, attaining a stationary growth phase at approximately 4 days. The doubling time was calculated to be about 12 to 15 h.

Isolation of kDNA. kDNAs were isolated as described (22) as networks from A_{15} cells at different passages (p). kDNAs from the wild type and from an arsenite-resistant variant with nuclear DNA amplification (A) at the highest dose of the drug (30 μM) were used as controls. Briefly, 2×10^{10} promastigotes at the stationary phase of growth for all passages were washed and lysed in 5 ml of lysis buffer (0.2 M NaCl, 10 mM Tris-HCl, 10 μM EDTA, and 1% sodium dodecyl sulfate [SDS; pH 8]). The lysates were passed through a 22-gauge needle, digested with proteinase K (100 μg ml^{-1}) at 42°C, and centrifuged for 1 h at 20,000 rpm (JA21 rotor; Beckman) to pellet the DNA networks. After extraction with phenol-chloroform-isoamyl alcohol (25:24:1 by volume), kDNAs were further purified by cesium chloride-ethidium bromide equilibrium ultracentrifugation. The lower band was isolated and stored in double-distilled H_2O after removal of the dye. The kDNAs were used within 30 days to prevent degradation. kDNAs from cells at the log phase of growth (2.5 days) during the transition period (i.e., cells at passages 26 and 27) were also isolated for comparison.

Dot blotting and Southern hybridization. Dot blots were prepared as described previously (30). A_{15} variants at different passages were washed with cold 0.15 M phosphate-buffered saline (pH 8.0) and adjusted to 2×10^8 cells ml^{-1}. Suspensions of parasites from each passage were serially 10-fold diluted, and 5 μl from each dilution was dot-blotted on a Nytran membrane (Schleicher & Schuell). Parasites from the wild type and the A variant, similarly diluted, served as controls. The blots were prehybridized and then hybridized with [^{32}P]DNA probes (Multiprime labeling system; Amersham) in the same solution (5× SSC [pH 7.4; 1× SSC is 0.15 M NaCl plus 0.015 M sodium citrate], 10× Denhardt's solution, 0.05 M sodium phosphate [pH 6.7], 0.5 mg of salmon sperm DNA ml^{-1}, 50% formamide) at 42°C. Blots were washed twice with 2× SSC containing 0.1% SDS for 15 min each at room temperature and then twice with 0.1× SSC containing 0.1% SDS for 30 min each at 60°C. They were then exposed to Kodak X-Omat film for 24 to 48 h with the use of an intensifying screen (DuPont). For the synthetic oligomer (see DNA probes), the probe was labeled with [γ-^{32}P]ATP by the end-labeling method (20). Prehybridization and hybridization of the blot were carried out in the same solution as described above except that the temperature was lowered to 37°C. Blots were washed with 5× SSC containing 0.1% SDS twice for 15 min each at room temperature and twice at 37°C with the same solution for 30 min each. The blots were exposed for 96 h.

DNA probes. The following DNA probes were used: pGWK1, a pGEM4Z plasmid carrying an 871-bp minicircle sequence cloned from wild-type *L. mexicana amazonensis* (13); pGAK1, a pGEM4Z plasmid carrying a 677-bp minicircle sequence specific for the minicircles of arsenite-resistant variants with DNA amplification (13); PT28, a pBR322 plasmid that contains a β-tubulin gene cloned from *L. mexicana amazonensis* (7); and a 22-mer, AACTGGGGGT TGGTGTAAAATA, which we synthesized, containing the universal origin of replication for all minicircles (underlined). This oligomer was shared with 100% identity between the wild-type- and A variant-specific minicircles (13).

Electron microscopy of kDNA networks. kDNA was spread out basically by the microdiffusion technique of Lang and Mitani (11) as described previously (13). Briefly, 2 μg of DNA in 0.1 ml of 0.15 M amonium acetate and 15 μg of cytochrome *c* per ml were mixed in a drop on Parafilm. The sample was picked up on 300-mesh grids coated with Parlodion film. The samples were stained with uranyl acetate in ethanol and rotary shadowed in platinum-palladium at an angle of 9°. Observations were made with a Zeiss 902 electron microscope.

Electron microscopy of ultrathin sections of kinetoplast. Washed promastigotes were fixed in 2.5% glutaraldelyde in 0.1 M cacodylate buffer (pH 7.3), postfixed in 1% OsO_4 in the same buffer for 20 min, rinsed in H_2O, and stained en bloc for 1 h with 1% aqueous uranyl acetate. After dehydration in a graded series of ethanol, samples were embedded in Spurr's resin (vinyl cyclohexene dioxide, 5 g ml^{-1}; DEP-736, 3 g ml^{-1}; nonenyl succinic anhydride, 10 g ml^{-1}; dimethylaminoethanol, 0.4 g ml^{-1}) and sectioned. The thin sections were stained with uranyl acetate and lead citrate and examined under an electron microscope (JEM 1200 EX; JEOL, Tokyo, Japan).

Decatenation of kDNA networks. kDNA networks were decatenated with calf thymus topoisomerase II. The enzyme, in a concentrated form in solution, was a generous gift from Leroy F. Liu, University of Medicine and Dentistry, New Jersey. In the final assay, 1 μg of kDNA was decatenated in the presence of a sufficient amount of topoisomerase in a final volume of 20 μl containing 50 mM Tris HCl (pH 7.6), 100 mM KCl, 10 mM $MgCl_2$, 0.5 mM dithiothreitol, 0.5 mM Na_2 EDTA, 0.5 mM ATP, and 30 μg of bovine serum albumin ml^{-1}. The reaction mixture was incubated at 30°C for 30 min. Decatenation of the kDNA networks was assessed by electrophoresis on 1% agarose gel. kDNA was then extracted once with phenol-chloroform-isoamyl alcohol (25:24:1 by volume), precipitated with ethanol, dried, and resuspended in TE buffer for electron-microscopic examination. The length of the DNA molecules was measured by tracing in a Macintosh computer with NIH Image 1.43 software. pBR322 (4,363 bp) and phage PM2 (10 kb) served as internal length controls.

RESULTS

Net loss of minicircles from kDNA network during the transition period of the switch of minicircle dominance. We have shown previously (13) that a switch in minicircle dominance occurred in arsenite-resistant variants growing at 10 μM arsenite when the arsenite concentration was raised to 15 μM during a serial stepwise selection for drug resistance. When kDNAs were isolated from 15 μM variants (A_{15} variants) at different passages (one passage [p] takes 4 days), the switch was observed to occur between passages 24 and 26 (24p and 26p). During this time, the number of predominant wild-type minicircles decreased rapidly while minicircles specific to arsenite-resistant variants with nuclear DNA amplification (A variant) gained dominance in the same kDNA network. Although gel electrophoresis and Southern analysis of kDNAs isolated from parasites at different passages clearly indicated a rapid transition during the switch, the results did not reflect the actual transition steps in the networks inside the parasites.

Therefore, A_{15} variants at different passages were dot blotted in serial 10-fold dilutions starting at 10^6 cells per well with the wild-type and A variants as controls. As can be seen

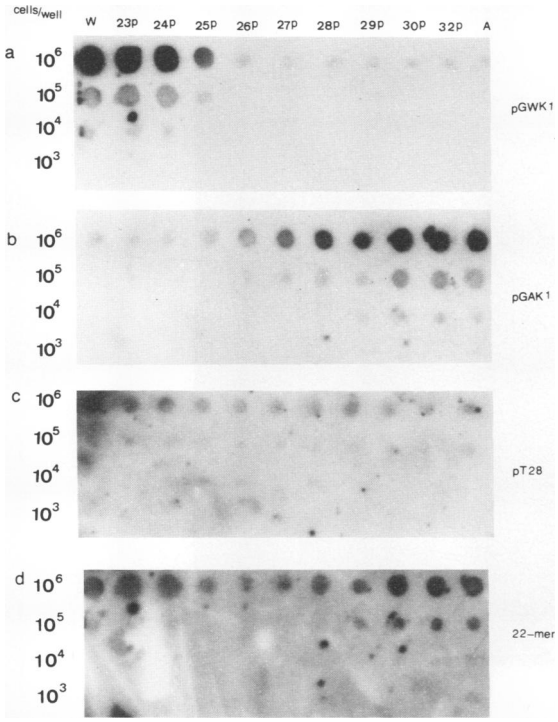

FIG. 1. Net loss of minicircles from *Leishmania* promastigotes during the transition of minicircle dominance. Parasites made resistant to 15 μM arsenite in a serial stepwise selection for drug resistance (A_{15} variant) were grown in the same concentration of the drug and passaged every 4 days. Parasites at different passages (as indicated by p) were dot blotted in serial 10-fold dilutions starting at 10^6 parasites per well onto a Nytran membrane and hybridized to cloned minicircles specific to either the wild type (pGWK1) or the A variant (pGAK1) on the same blot after washing. PT28, a cloned tubulin gene from *L. mexicana amazonensis*, served as an internal control. A 22-mer shared with 100% identity between wild-type- and A variant-specific minicircles was synthesized and used as a common probe (see DNA probes in Materials and Methods) for both minicircle classes. W, wild-type cells; A, arsenite-resistant variants (resistant to 30 mM arsenite) with DNA amplification.

TABLE 1. Densitometric measurements of hybridization intensity of the dots shown in Fig. 2

Source of cells	Density of dots (%) compared with[a]:	
	Wild type (W)	A variant
W	40.0 (100)	0.12 (0.45)
23p	38.5 (96)	0.09 (0.33)
24p	35.1 (88)	0.18 (0.60)
25p	13.64 (34)	0.67 (2.40)
26p	0.98 (2.4)	3.11 (11.4)
27p	0.37 (0.90)	6.40 (23.5)
28p	0.08 (0.20)	12.58 (46)
29p	0.11 (0.28)	18.2 (66.9)
30p	0.12 (0.31)	25.6 (94)
32p	0.10 (0.25)	27.1 (99.9)
A	0.11 (0.29)	27.2 (100)

[a] The density of dots was measured by densitometry. Each measurement is the average of three point measurements on each dot. Percentages were calculated for each passage compared with the wild type (W) and the A variant.

from Fig. 1a, when wild-type-specific minicircle pGWK1 was used as the probe (see DNA probes in Materials and Methods), the predominant wild-type minicircles decreased in copy number starting at 25p and quickly reached a very low level after the 27p compared with the wild-type control (W). Meanwhile, when A variant-specific minicircle pGAK1 was used as the probe, A variant-specific minicircles were present in increasing levels starting at 25p and reached a stable level similar to that of the A variant (A) only at 28p (Fig. 1b). Obviously there was a time during the transition from wild-type minicircles to the A variant-specific minicircles in which neither the wild-type nor the A variant-specific minicircles were present in normal copy numbers. This was especially true for minicircles in cells at 26p and 27p. Use of probe PT28, a cloned tubulin gene which served as the internal control (Fig. 1c), indicated that approximately equal numbers of parasites were applied to each well.

Densitometric measurements of dots from Fig. 1a and b showed that the level of wild-type minicircles had indeed dropped by more than 65% at 25p, by 97.6% at 26p, and by more than 99% at 27p, compared with W (Table 1). The level of wild-type minicircles remained at 0.2 to 0.3% of the wild-type control level thereafter. The A variant-specific minicircles in the wild-type cells and in the variants at 23p and 24p amounted to 0.3 to 0.6% of the level in the A variant control (Table 1). The level did not attain that of the A variant until the 30p to 32p. Thus the number of A variant-specific minicircles gradually climbed from 25p until 30p to reach the A variant level, while the number of wild-type-specific minicircles rapidly declined from 25p to 26p.

A 22-mer which was shared with 100% identity between the wild-type- and A variant-specific minicircles (see DNA probes in Materials and Methods) was synthesized for use as a common probe to verify the decrease of wild-type minicircles and the increase of A variant-specific minicircles during the transition. Indeed, the minicircle copy numbers decreased in parasites at 25p, 26p, and 27p, reflecting the true loss of minicircles from these parasites (Fig. 1d).

Ultrastructural analysis of the kDNA networks during the transition period. Single kDNA networks of wild-type *L. mexicana amazonensis* spread out by the microdiffusion technique showed that the network consisted of many topologically interlocked or catenated minicircles forming an oval sheet 12 μm long and 8.7 μm wide (average measurements from 15 sheets) (Fig. 2, W). In addition to the minicircle components, longer DNA could be seen protruding from the edge of the sheet, representing maxicircles (arrowheads). Very long DNA fibrils (LDFs) (arrows) were seen threading through the interior and around the rim of the sheet. The networks isolated from 24p and 25p (Fig. 2, 24–25p) were comparable in size (approximately 12.4 by 8.5 μm, average measurements from 16 sheets per passage) to those of the wild type. However, they had relatively fewer minicircles, and the LDFs (arrows) were more prominent and generally thicker in appearance than the maxicircle edge loops (arrowheads). The sheets at 26p and 27p (Fig. 3) differed in shape and size from those of the wild type (approximately 11.96 by 5.98 μm for 26p and 12.2 by 6.04 μm for 27p; 18 sheets measured per passage). The whole network was loosely packed and irregularly shaped. The sheet at 26p was almost devoid of minicircles, exposing large open spaces inside it. The LDFs were very prominent, running from one end of the sheet to the other, seemingly forming the backbone or skeleton of the network. Thinner DNA threads representing maxicircles formed edge loops or threaded inside the sheet, possibly catenated with the LDFs (arrow-

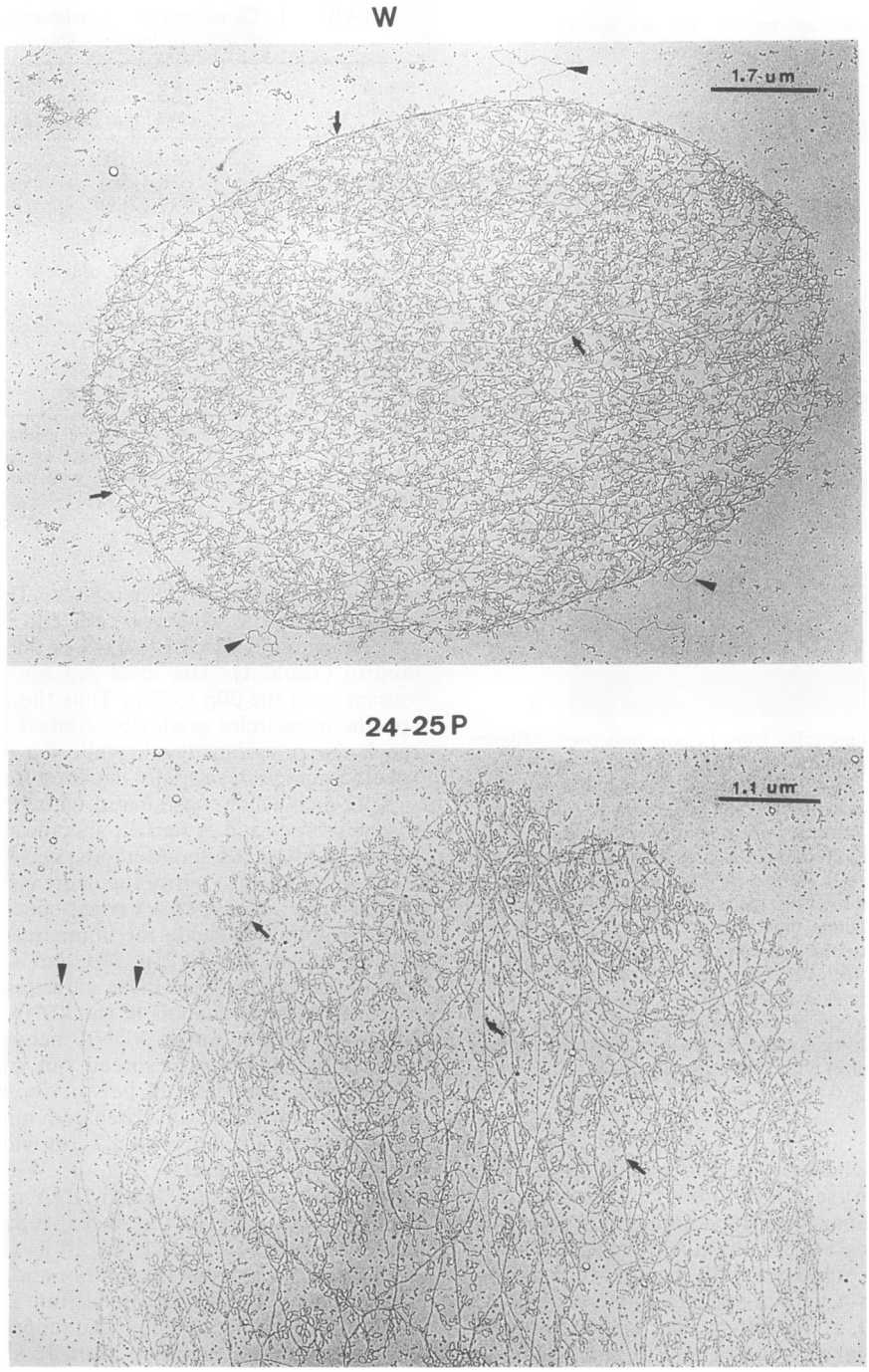

FIG. 2. Electron micrographs of kDNA networks from the wild type (W) and A_{15} variants at passages 24 to 25 (24–25P). Arrow, LDFs; arrowhead, maxicircle side loops. For panel W, bar, 1.7 μm; magnification, ×7,000. For panel 24–25P, bar, 1.1 μm; magnification, ×7,000.

heads). Almost no minicircles were found attached to the thinner maxicircle DNAs. Wherever minicircles were found, they were attached to the LDFs. The sheet at 27p appeared very similar to that at 26p, except that minicircle aggregates were forming in some areas. These aggregates were probably formed through catenation of minicircles (Fig. 3, open triangles at 27p). Sheets at 28p to 32p (Fig. 4) (12.1 by 8.4 μm, 12 sheets measured at 28p) were generally gaining a regular oval shape with minicircles catenating around the periphery of the sheet. The sheet shown for 32p represents a sheet with a loosened bottom whose rim has curled upward to give the appearance of a shoe. This structure could be found in other preparations too and has been described by other researchers previously (1). However, large interior open spaces were still features of these networks.

kDNA networks isolated from the log phase cells at 26p

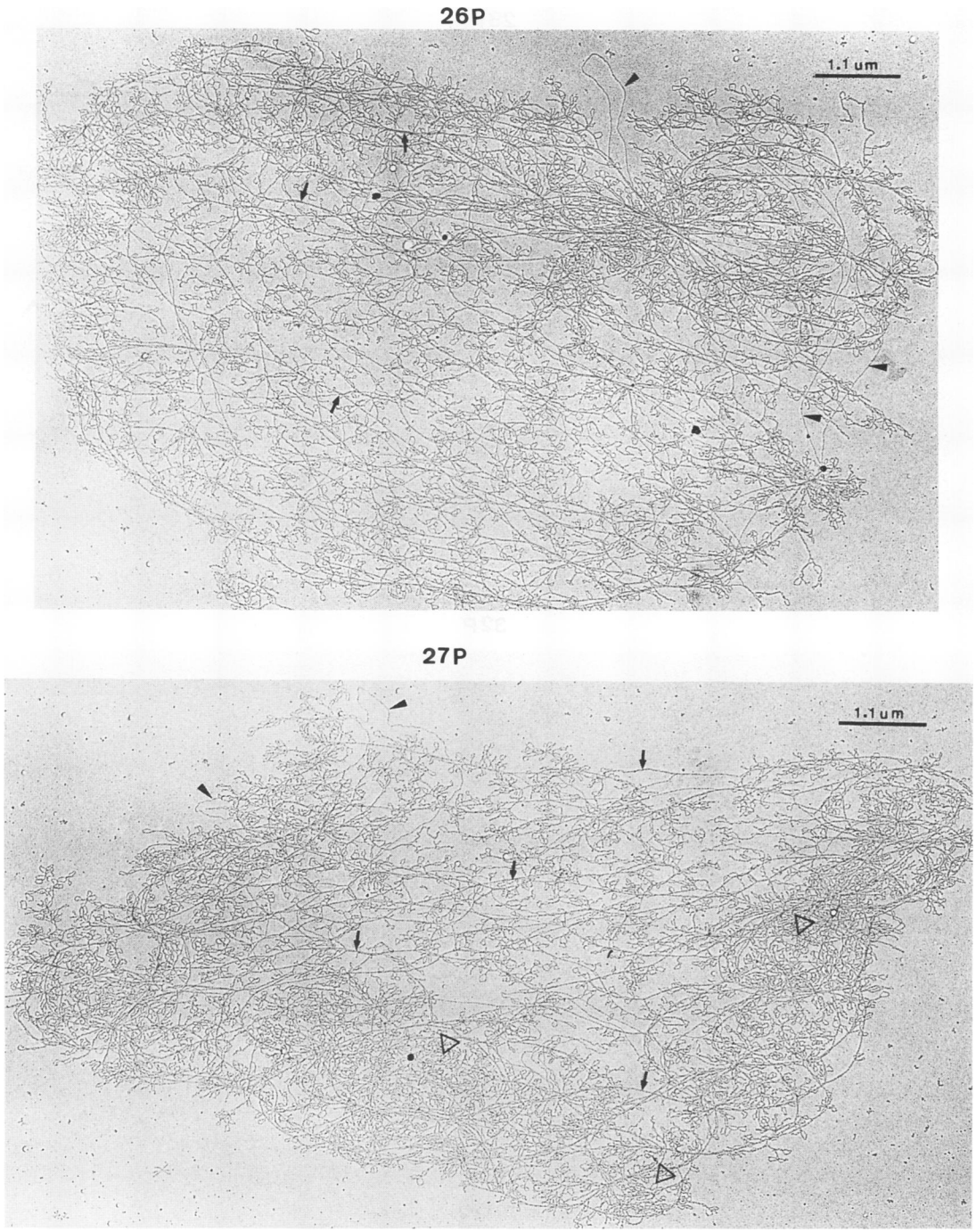

FIG. 3. Electron micrographs of kDNA networks isolated from A_{15} variants at passages 26 (26P) and 27 (27P). See the legend to Fig. 2 for definitions of arrows and arrowheads. Open triangle, minicircle aggregates; bar, 1.1 μm; magnification, ×7,000.

and 27p (2.5 days after the passage) were examined for comparison with those at stationary phase. The structures of these networks were not different from those isolated from stationary-phase cells at 26p and 27p (compare Fig. 5b with networks in Fig. 3, 26p and 27p). They were still characterized by large interior open spaces. Similarly isolated networks from wild-type log-phase cells appear to have some empty spaces inside the network (Fig. 5a); this may be due to loss of replicating minicircles from these networks. The composition of the minicircles in the wild-type networks, however, appears to be quite different from that of variants at 26p and 27p (compare Fig. 5a and b).

Electron microscopy of the ultrathin sections of the kinetoplasts during the transition period. Figure 6 shows ultrathin cross-sections of kDNA from the kinetoplast regions of the variants described in Fig. 2 to 4. The kDNA network of the wild-type (W) cells appeared to be an electron-dense concave body with fibrous materials (kDNA) surrounded by an

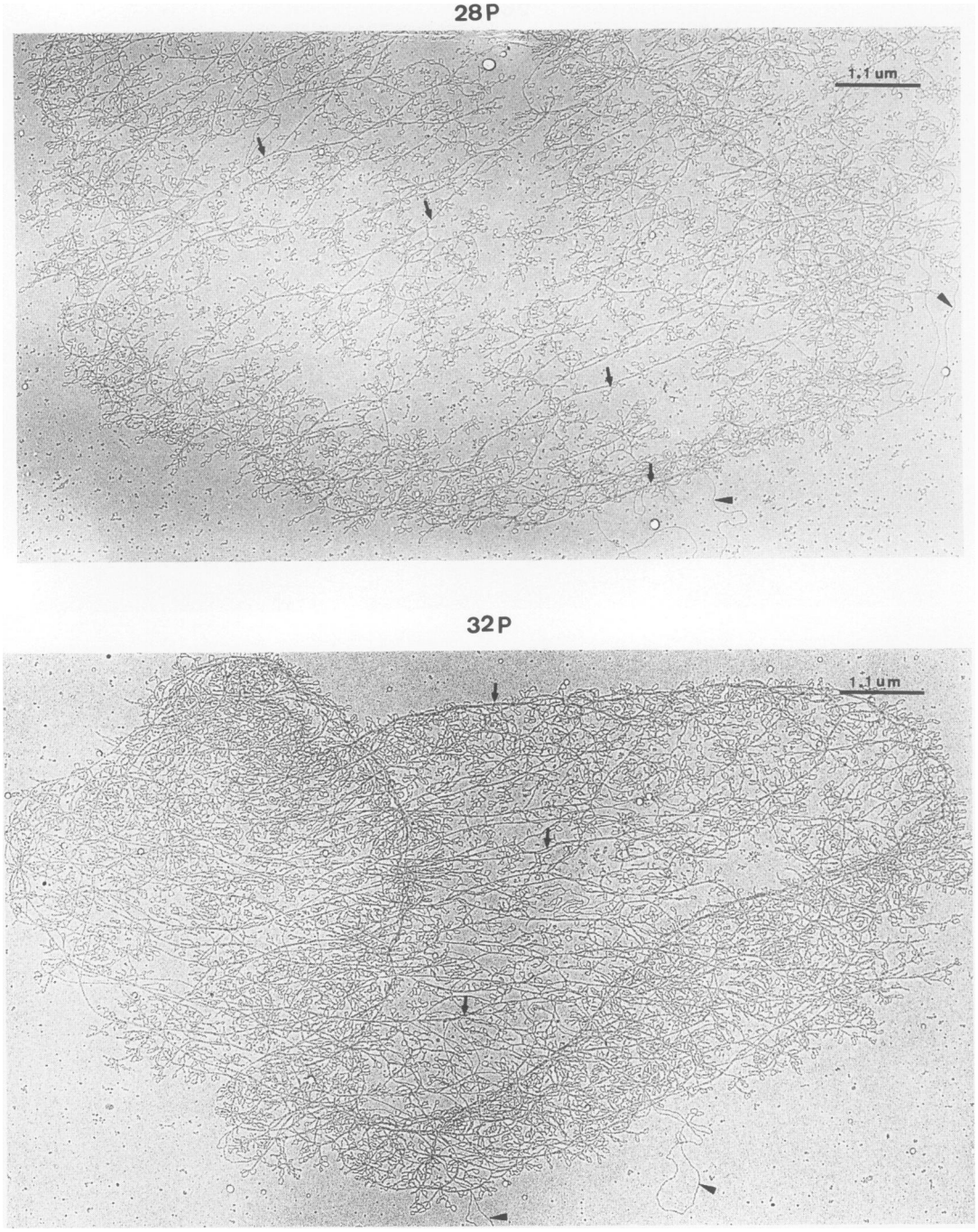

FIG. 4. Electron micrographs of kDNA networks isolated from A_{15} variants at passages 28 (28P) and 32 (32P). See the legend to Fig. 2 for definitions of arrows and arrowheads. Bar, 1.1 μm; magnification, ×7,000.

intact mitochondrial membrane (M), situated at the basal region of the flagellum (B). This is in accordance with results of other studies (1, 23). The networks from 24p to 25p appeared almost the same as those in the wild type. However, the electron density at 26p (Fig. 6, 26Pa, 26Pb, and 26Pc) and 27p (Fig. 6, 27Pa and 27Pb) was greatly reduced to become almost transparent in some areas, giving a window-like appearance along the length of the cross-sectioned kDNA network. The appearance of the clear spaces in kDNA ultrathin sections coincided with the reduced concentration of minicircles as observed by dot hybridization of the cells (Fig. 1) and with the loss of most minicircles from the sheets at 26p and 27p (Fig. 3). The open spaces became smaller at 28p, and the kinetoplast kDNAs regained normal electron density only by the 30p to 32p. These results showed that the events observed in the networks in Fig. 2 to 4 were not likely to be due to in vitro artifacts.

Ultrastructural study of kDNA networks after treatment

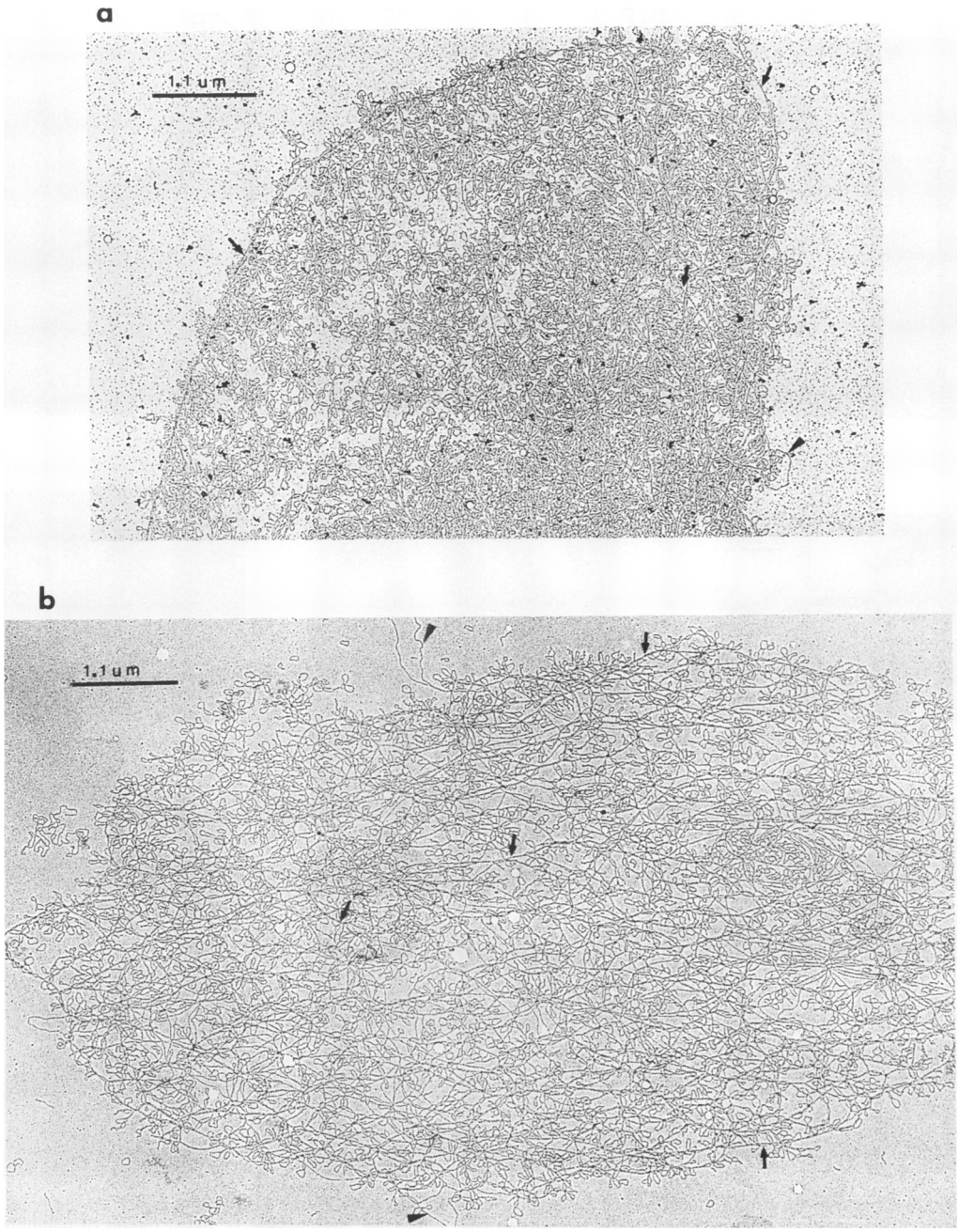

FIG. 5. Electron micrographs of kDNA networks isolated from log-phase cells. (a) kDNA network from log phase wild type (bar, 1.1 μm; magnification, ×7,000). (b) kDNA network from 26P variant at log phase (bar, 1.1 μm; magnification, ×7,000). For definitions of arrows and arrowheads, see the legend to Fig. 2.

with calf thymus topoisomerase II. kDNA networks from wild-type and A_{15} variants at 26p were completely decatenated by calf thymus topoisomerase II when assessed by electrophoresis on a 1% agarose gel (data not shown). Four types of DNA molecules were often seen, monomeric maxicircles and minicircles and long and short linear DNA molecules. Figure 7a shows a field from 26p kDNA after decatenation; a maxicircle (arrowhead), a long linear DNA fibril (arrow), a few short linear DNA molecules (double arrows), and a few minicircles or minicircle aggregates (double arrowheads) are seen. Figure 7b shows two free maxicircles from kDNA of the same passage. Figure 7c shows a field of decatenated wild-type kDNA, where some short linear DNAs and minicircles are seen scattered around a single maxicircle (arrowhead). Long linear DNA molecules two to four times the length of maxicircles were observed more frequently in topoisomerase-treated samples than in nontreated samples. However, the mere presence of long linear DNA molecules in the topoisomerase-nontreated samples makes it difficult to pinpoint their exact origins. The minicircles were averaged 0.278 ± 0.04 μm in length (aver-

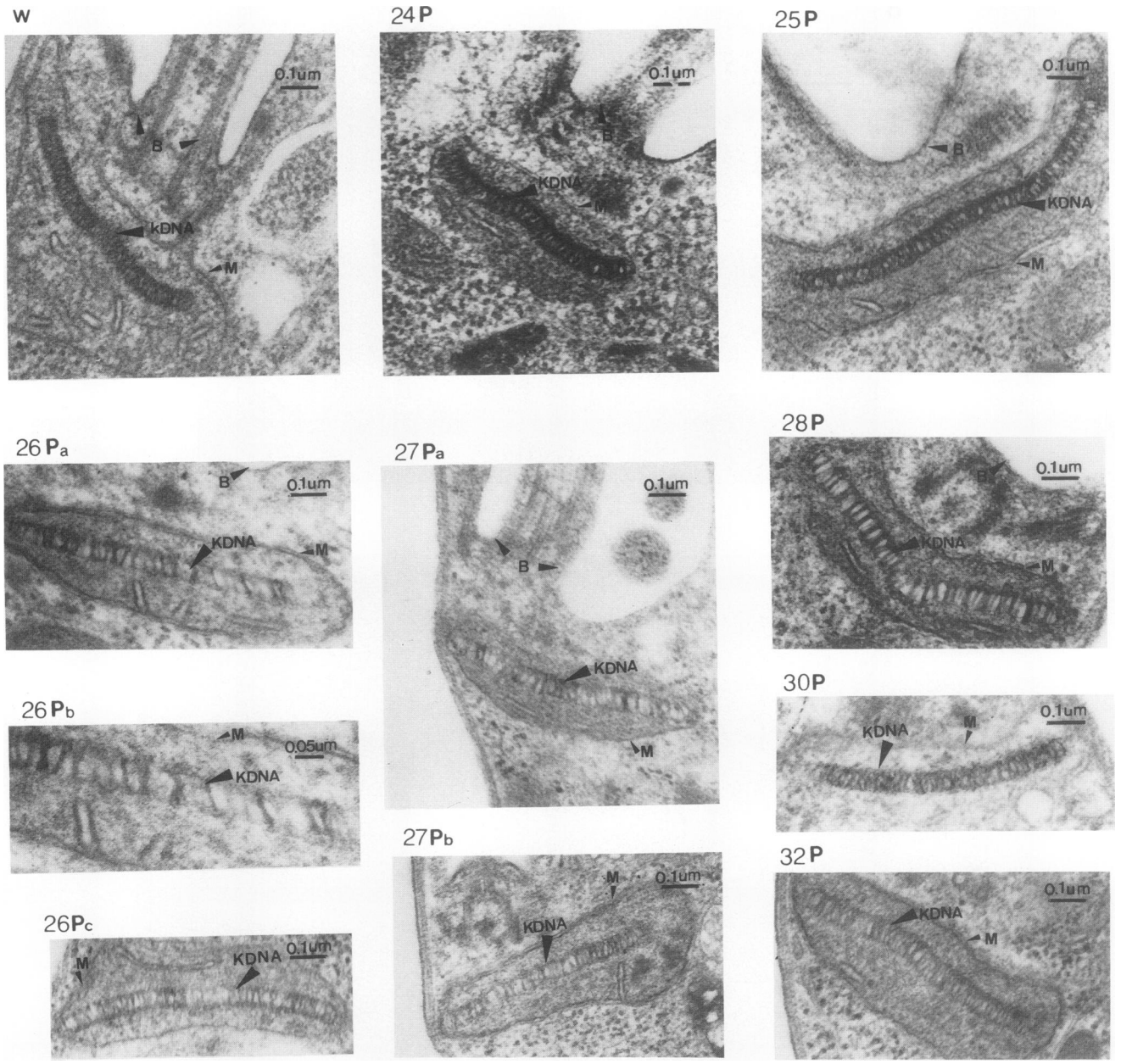

FIG. 6. Electron micrographs of ultrathin sections of *L. mexicana amazonensis* from the kinetoplast region of the wild type (W) and its A_{15} variants at different passages (P) as described in the legends to Fig. 1 to 4. M, membrane; B, basal region of flagellum; bars, 0.1 μm; magnification, ×60,000 (except for 26Pb: bar, 0.05 μm; magnification, ×100,000).

age of 74 minicircles), and maxicircles were 7.31 ± 0.7 μm long (average of 21 maxicircles).

DISCUSSION

Molecular analyses combined with ultrastructural studies not only enabled us to observe step by step the molecular changes taking place in minicircles within kDNA networks during the transition period but also allowed us for the first time to see clearly the structural organization of the network in a natural setting. In addition to minicircles and maxicircles, the kDNA network contains within it many LDFs running from one end of the network to the other, seemingly forming a frame for the network; these LDFs were revealed after the network had lost almost all the wild-type-specific minicircles at the 26p and 27p passages (Fig. 2; Table 1). This stage was followed immediately by gradual replication of minor variant-specific minicircles in the same network. The variant-specific minicircle copy numbers increased gradually, starting probably from the periphery of the sheet (Fig. 3, 27p, and Fig. 4, 28p), to fill the large open spaces created by the loss of wild-type minicircles. This sheet-mending process was not completed until 30p (Table 1). During the mending process, minicircles catenate among themselves, thus possibly constituting the primary stabilizing force for the kDNA network by forming aggregates (Fig. 4, open

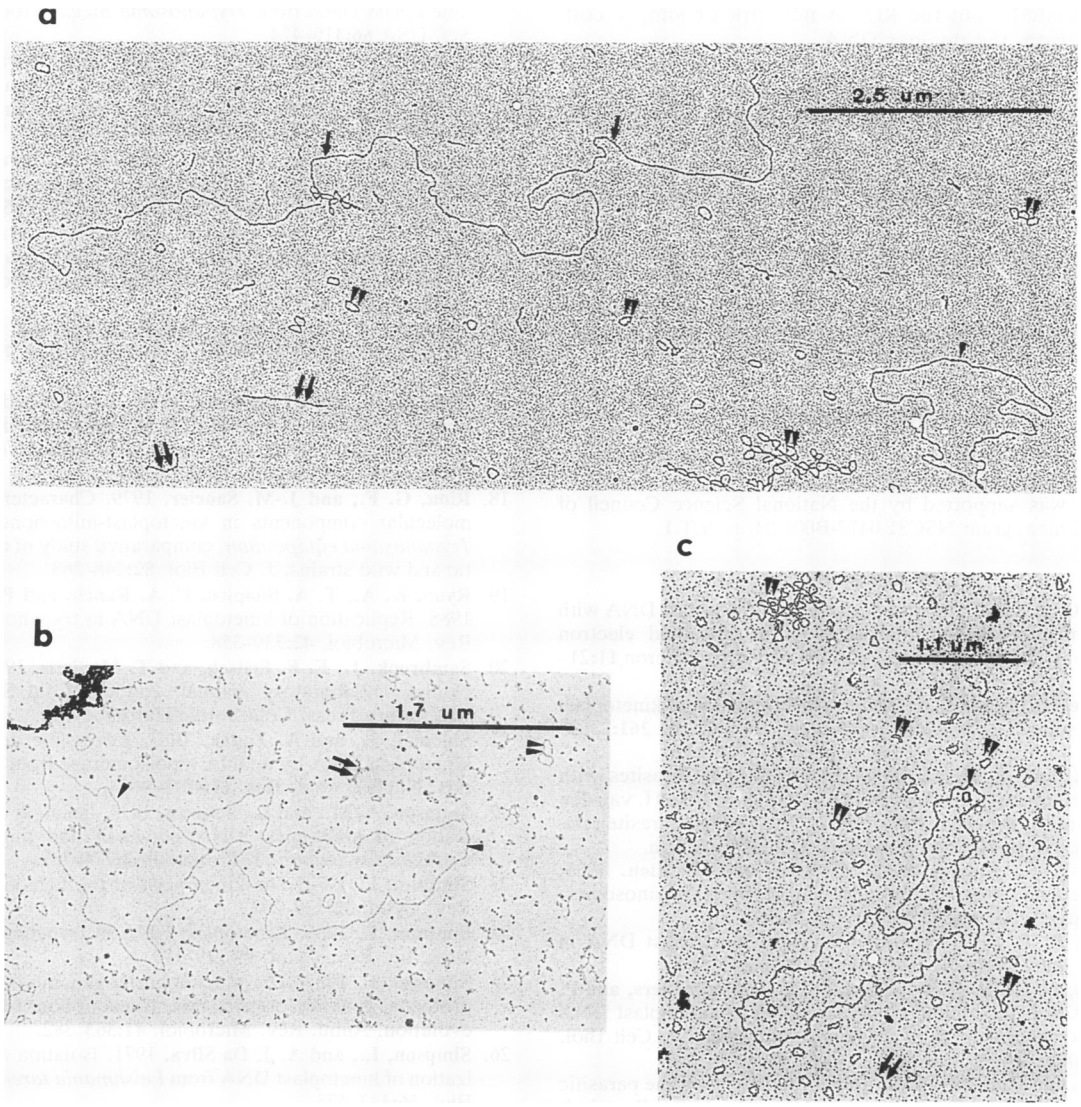

FIG. 7. Electron micrographs of calf thymus topoisomerase II-treated kDNA networks. (a) A field of kDNA network components from variants at 26p after decatenation (bar, 2.5 μm; magnification, ×3,000). (b) Two maxicircles decatenated from networks at 26p (bar, 1.7 μm; magnification, ×4,400). (c) kDNA network components from wild-type cells after decatenation (bar, 1.1 μm; magnification, ×7,000). Arrow, long LDF; double arrow, shorter linear DNA molecule; arrowhead, maxicircles; double arrowheads, minicircles and their catenanes.

triangles). No minicircles were found attached to the thinner maxicircle DNA strands. However, the maxicircles may constitute a secondary stabilizing force through catenation with LDFs to prevent the network from falling apart when most of the minicircles (86%) are lost (Fig. 3, 26p).

Minicircles are known to be released from the network during replication (2, 5, 19), and such a process would create empty spaces inside the network. Some kDNA networks from wild-type parasites appeared to have empty spaces in the sheet during log-phase growth (Fig. 5a), which may have been due to loss of replicating minicircles. However, these networks were quite different in appearance from those seen in variants at 26p and 27p at the same log phase, in which the empty spaces were distributed evenly across the whole network (Fig. 5b). The structure of the networks in variants at 26p and 27p during log phase growth was not different, however, from their structure during the stationary phase (compare Fig. 5b with Fig. 3 at 26p and 27p). This observation indicates that the process of loss of dominant minicircles from these networks during the transition period differs from the loss of minicircles in the wild-type cells during replication.

The nature of the LDFs is not clear. Their presence appears to be necessary to provide a supporting framework to maintain network structure when 76 to 86% of minicircles are lost (Fig. 2, 26p and 27p) during the transition period. Such a support would allow minicircles and maxicircles to replicate since we found that both these circular DNAs associate with the LDFs. Decatenation by topoisomerase II revealed the presence of some long linear DNA molecules two to four times the length of the maxicircles in the kDNA preparation. Linear DNA molecules in kDNA preparations have also been described previously by others (1, 16). Since long linear DNA molecules were sometimes found in samples without topoisomerase treatment, it is not clear whether these long DNA molecules represent a different class of

DNA dissociated from the kDNA network or simply contaminations from the nuclear DNA.

A network structure that contains very few minicircles (Fig. 2, 26p) helps to differentiate transkinetoplastidy as we proposed it (11) from dyskinetoplastidy (9, 17, 18, 29). In the former phenomenon as we view it, the presence of a kinetoplast skeleton without minicircles is important for the regeneration of the network and probably also for its function. In dyskinetoplastidy, the network structure is dissociated so much that the net-mending process cannot re-form the network. This report reveals the organization of the kDNA network in detail; the relationships between the individual components and their physical arrangements within the network require further investigation.

ACKNOWLEDGMENTS

We are grateful to Lola Wen for her excellent secretarial work and to Cathy Fletcher for reading the manuscript.

This work was supported by the National Science Council of Republic of China, grant NSC81-0412-B001-04, to S.T.L.

REFERENCES

1. **Barker, D. C.** 1980. The ultrastructure of kinetoplast DNA with particular reference to interpretation of dark field electron microscopy images of isolated purified networks. Micron **11**:21–62.
2. **Birkenmeyer, L., and D. S. Ray.** 1986. Replication of kinetoplast DNA in isolated *Crithidia fasciculata*. J., Biol. Chem. **261**:2362–2368.
3. **Borst, P., and A. H. Fairlamb.** 1976. DNA of parasites with special reference to kinetoplast DNA, p. 169–191. *In* H. van den Bossche (ed.), Biochemistry of parasites and host-parasite relationships. North-Holland Publishing Co., Amsterdam.
4. **Douc-Rasy, S., A. Kayser, J. F. Riou, and G. Riou.** 1986. ATP-independent type 11 topoisomerase from trypanosomes. Proc. Natl. Acad. Sci. USA **83**:7152–7156.
5. **Englund, P. T.** 1979. Free minicircles of kinetoplast DNA in *Crithidia fasciculata*. J. Biol. Chem. **254**:4895–4990.
6. **Fairlamb, A. H., P. O. Weislogel, J. H. J. Hoeijmakers, and P. Borst.** 1978. Isolation and characterization of kinetoplast DNA from bloodstream form of *Trypanosoma brucei*. J. Cell Biol. **76**:293–309.
7. **Fong, D., and D. B. Lee.** 1988. Beta tubulin gene of the parasitic protozoan *Leishmania mexicana*. Mol. Biochem. Parasitol. **31**:97–106.
8. **Fouts, D. L., D. R. Wolstenholme, and H. W. Boyer.** 1978. Heterogeneity in sensitivity to cleavage by the restriction endonucleases EcoR1 and HindIII of circular kinetoplast DNA molecules of *Crithidia acanathocephali*. J. Cell Biol. **79**:329–341.
9. **Hajduk, S. L., and W. B. Cosgrove.** 1979. Kinetoplast DNA from normal and dyskinetoplastic strains of *Trypanosoma equiperdum*. Biochim. Biophys. Acta **561**:1–9.
10. **Kleisen, C. M., P. Borst, and P. J. Weijers.** 1976. The structure of kinetoplast DNA. I. The mini-circles of *Crithidia lucillae* are heterogeneous in base sequence. Eur. J. Biochem. **64**:141–151.
11. **Lang, D., and M. Mitani.** 1970. Simplified quantitative electron microscopy of biopolymers. Biopolymers **9**:373–379.
12. **Laurent, M., and M. Steinert.** 1970. Electron microscopy of kinetoplast DNA from *Trypanosoma mega*. Proc. Natl. Acad. Sci. USA **66**:419–424.
13. **Lee, S. T., C. Tarn, and K. P. Chang.** 1993. Characterization of the switch of kinetoplast DNA minicircle dominance during development and reversion of drug resistance in *Leishmania*. Mol. Biochem. Parasitol. **58**:187–204.
14. **Lee, S. T., C. Tarn, and C. Y. Wang.** 1992. Characterization of the sequence changes in kinetoplast DNA maxicircles in drug-resistant *Leishmania*. Mol. Biochem. Parasitol. **56**:197–208.
15. **Lee, S. Y., S. T. Lee, and K. P. Chang.** 1992. Transkinetoplastidy—a novel phenomenon involving bulk alterations of mitochondrion-kinetoplast DNA of a trypanosomatid protozoa. J. Protozool. **39**:190–196.
16. **Marini, J. C., K. G. Miller, and P. T. Englund.** 1980. Decatenation of kinetoplast DNA by topoisomerases. J. Biol. Chem. **255**:4976–4979.
17. **Riou, G. F., and R. Pautrizel.** 1977. Isolation and characterization of circular DNA molecules heterogeneous in size from a dyskinetoplastic strain of *Trypanosoma equiperdum*. Biochem. Biophys. Res. Commun. **79**:1084–1091.
18. **Riou, G. F., and J.-M. Saucier.** 1979. Characterization of the molecular components in kinetoplast-mitochondrial DNA of *Trypanosoma equiperdum*, comparative study of dyskinetoplastic and wild strains. J. Cell Biol. **82**:248–263.
19. **Ryan, K. A., T. A. Shapiro, C. A. Ranch, and P. T. Englund.** 1988. Replication of kinetoplast DNA in trypanosomes. Annu. Rev. Microbiol. **42**:339–358.
20. **Sambrook, J., E. F. Fritsch, and T. Maniatis.** 1989. Molecular cloning: a laboratory manual, 2nd ed. Cold Spring Harbor Laboratory Press, Cold Spring Harbor, N.Y.
21. **Shlomai, J., and A. Zodak.** 1983. Reversible decatenation of kinetoplast DNA by a DNA topoisomerase from trypanosomatids. Nucleic Acids Res. **11**:4019–4034.
22. **Simpson, A. M., and L. Simpson.** 1974. Isolation and characterization of kinetoplast DNA networks and minicircles from *Crithidia fasciculata*. J. Protozool. **2**:774–781.
23. **Simpson, L.** 1972. The kinetoplast of the hemoflagellates. Int. Rev. Cytol. **32**:139–207.
24. **Simpson, L.** 1986. Kinetoplast DNA in trypanosomatid flagellates. Int. Rev. Cytol. **99**:119–179.
25. **Simpson, L.** 1987. The mitochondrial genome of kinetoplastid protozoa, genomic organization, transcription, replication, and evolution. Annu. Rev. Microbiol. **41**:363–382.
26. **Simpson, L., and A. J. Da Silva.** 1971. Isolation and characterization of kinetoplast DNA from *Leishmania tarentolae*. J. Mol. Biol. **56**:443–473.
27. **Steinert, M., S. van Assel, and G. Steinert.** 1976. Minicircular and non-minicircular components of kinetoplast DNA, p. 193–202. *In* H. van den Bossche (ed.), Biochemistry of parasites and host-parasite relationships. North-Holland Publishing Co., Amsterdam.
28. **Stuart, K.** 1983. Kinetoplast DNA, mitochondrial DNA with a difference. Mol. Biochem. Parasitol. **9**:93–104.
29. **Vickerman, K., and T. M. Preston.** 1976. Comparative cell biology of the kinetoplastid flagellates, vol. 1., p. 35–130. *In* W. H. R. Lumsden and D. A. Evans (ed.), Biology of the Kinetoplastidae. Academic Press, Inc., New York.
30. **Wirth, D. F., and D. M. Pratt.** 1982. Rapid identification of *Leishmania* species by specific hybridization of kinetoplast DNA in cutaneous lesions. Proc. Natl. Acad. Sci. USA **79**: 6999–7003.